

Rubrique: Ondes élastiques

Seismic response of a set of blocks partially imbedded in soft soil

Titre courant: Seismic response of a set of blocks

Réponse sismique d'un ensemble de blocs partiellement encastrés dans un terrain mou

Chrysoula TSOGKA and Armand WIRGIN

Laboratoire de Mécanique et d'Acoustique, UPR 7051 du CNRS, 31 chemin Joseph Aiguier, 13402 Marseille cedex 20, France.

E-mail: tsogka@lma.cnrs-mrs.fr, wirgin@lma.cnrs-mrs.fr

Auteur correcteur des épreuves: Armand WIRGIN, Laboratoire de Mécanique et d'Acoustique, UPR 7051 du CNRS, 31 chemin Joseph Aiguier, 13402 Marseille cedex 20, France. N° tel.: 04 91 16 40 50, N° Fax: 04 91 22 08 75, E-mail: wirgin@lma.cnrs-mrs.fr

Abstract

The seismic response of a set of ten non-equally spaced, non-equally sized, homogeneous blocks partially imbedded in a soft soil layer overlying a hard halfspace is studied numerically and shown to be generally larger, in terms of amplitude, duration and spatial variability than that of the ground in the presence of one block or in the absence of blocks. This is qualitatively similar to observed seismic response in the past at sites such as Mexico City and suggests that the built portion of cities may, under certain conditions, play a significant role in the global seismic response of a city.

Résumé

On étudie numériquement la réponse sismique d'un ensemble de dix blocs, dissemblables, non équiésespacés et ancrés dans une couche molle au-dessus d'un demi-espace dur, et on montre qu'elle est généralement plus importante, en termes d'amplitude, durée et variabilité spatiale que la réponse au niveau du sol en présence d'un seul bloc ou en l'absence de blocs. Ceci est qualitativement en accord avec la réponse sismique constatée dans le passé dans des villes telles que Mexico et indique que la partie bâtie peut, dans certaines conditions, jouer un rôle significatif dans la réponse sismique globale d'une ville.

Keywords: earthquakes, cities

Mots-clés: tremblements de terre, villes

Version française abrégée

On étudie numériquement les solutions du système d'équations (1), relatif à la propagation d'ondes élastiques SH dans une configuration 2D (représentée dans la Fig.1) constituant une approximation grossière d'une ville, comportant un ensemble de structures bâties sous forme de blocs non équiespacés, de formes et tailles non-identiques, partiellement encastrés dans une couche molle au-dessus d'un massif rocheux. Cette structure est soumise à l'onde rayonnée par une source linéique impulsionnelle donnée par (3) et (4) et il s'agit d'en calculer la réponse afin d'essayer de rendre compte des réponses sismiques anormales déjà observées et/ou attendues dans des villes telles que Kobe [1] (Japon), Izmit [2] (Turquie), Nice [3], Mexico [4-6], Los Angeles [7-9] etc., qui ont la particularité d'être toutes bâties sur terrain mou, sachant que la réponse est qualifiée de 'normale' en l'absence des blocs (i.e., la surface libre constituée par le sol est plane, le sous-sol étant encore comme dans la Fig.1). En effet, le modèle 1D [10], rendant compte de la réponse 'normale' (Fig. 4), ne prévoit pas les battements de signal, les codas très prolongées de mouvement, la variabilité spatiale de réponse, qui en termes de mouvement crête, peut être importante, observés à maintes reprises dans des sites tels que Mexico [5,6].

Nos calculs, issus d'une méthode numérique [13-18], dite de type 'domaine fictif', employant des éléments finis en espace et des différences finies en temps, incorporant une PML [15] pour fermer le domaine infini sans engendrer des réflexions parasites, et faisant appel à une technique efficace pour rendre compte de la condition de surface libre sur le sol et les parties affleurantes dans l'air des blocs (Fig. 2) , ont permis de montrer que les blocs agissent comme des éléments diffringents permettant d'exciter localement des modes ou quasi-modes de Love [11,12,19], dont la traduction au niveau des blocs (qui possèdent leurs propres systèmes de modes, modifiés par couplage aux modes de Love) et dans leur voisinage est une réponse (Fig.3) dont les caractéristiques sont qualitativement semblables à celles évoquées plus haut dites 'anormales'. Ceci indique que la partie bâtie peut, dans certaines conditions, jouer un rôle significatif dans la réponse sismique d'ensemble d'une ville et suggère comment analyser (et prédire) les destructions dans des villes réelles soumises à des tremblements de terre anciens (et futurs).

1 Introduction

A noticeable feature of many cities, such as Kobe [1] (Japan), Izmit [2] (Turkey), Nice [3] (France), Mexico City [4-6], Los Angeles [7-9] etc., in which significant damage has occurred (and/or is expected to occur) during earthquakes, is that they are partially or wholly built on soft soil. A straightforward 1D analysis [10] (that takes no account of the presence of the buildings) shows that the soft layer increases the seismic vulnerability of the city in that it is responsible for amplification of ground motion during an earthquake. However, the 1D model does not account either for the beating phenomena and very long codas in the building vibrations, nor for the large spatial variability of response, which, in terms of peak motion can be large, repeatedly observed in sites such as Mexico City [5,6].

These puzzling effects kindled the present study of the action of a seismic wave on a relatively-simple structural model (albeit more general than the one studied in [11,12]) with both geological and man-made features. This 2D model has three components (from bottom to top in Fig.1): a hard half space (HHS), overlaid by a soft soil layer (SL), in which are partially imbedded a set of even softer blocks (SB). HHS and SL are geological features, the set of SB is man-made and constitutes a very crude representation of the built features (buildings, blocks of buildings, etc.) of a city.

2 Basic ingredients of the analysis

The structure is invariant in the y -direction with x, y, z the cartesian coordinates, and z increasing with depth (see Fig.1 wherein the x - z sagittal plane is displayed). The seismic source is a line in the y -direction, radiating a Ricker pulse cylindrical shear-horizontal (SH) displacement field. Thus, only the y -component of this field is non-vanishing and invariant with respect to y and gives rise to a total field underneath and on the free surface which is also SH -polarized and invariant with respect to y . The resulting problem is 2D with the displacement field depending only on x, z and on time t . In Fig. 1 we denote by h, w and d , the height, width and space interval between blocks. We consider h, w and d to vary from one block to another. The half-space underneath the irregular stress-free surface is occupied by a linear, isotropic, *heterogeneous* medium, characterized by mass density $\rho(\mathbf{x})$ and shear modulus $\mu(\mathbf{x})$, $\mathbf{x} = (x, z)$. Both $\rho(\mathbf{x})$ and $\mu(\mathbf{x})$ are considered to be positive real, piecewise constant, time-invariant functions. Thus, no intrinsic medium losses are taken into account. Moreover, the blocks are homogeneous and filled with the same material.

The governing equations for the propagation of 2D SH -waves in heterogeneous solids are, in the mixed first-order formulation:

$$\begin{aligned} \frac{\partial \mathbf{v}(\mathbf{x}, t)}{\partial t} + \mu(\mathbf{x}) \nabla u(\mathbf{x}, t) &= 0 \\ \rho(\mathbf{x}) \frac{\partial u(\mathbf{x}, t)}{\partial t} + \nabla \cdot \mathbf{v}(\mathbf{x}, t) &= \rho(\mathbf{x}) g(\mathbf{x}, t) \end{aligned} \quad , \quad \mathbf{x} \in \mathbf{R}^2, \quad t \in \mathbf{R}^+ . \quad (1)$$

wherein g is a driving function, u the y -component of the displacement field, and $\partial_t \mathbf{v} = -(\sigma_{yx}, \sigma_{yz})$. By taking the divergence of the first of these two equations, the partial time-derivative of the second equation, and subtracting the two expressions so obtained, one is led to the standard wave equation for propagation of SH waves in a heterogeneous solid

$$\mu(\mathbf{x}) \nabla \cdot \nabla u(\mathbf{x}, t) + \nabla \mu(\mathbf{x}) \cdot \nabla u(\mathbf{x}, t) - \rho(\mathbf{x}) \frac{\partial^2 u(\mathbf{x}, t)}{\partial t^2} = -\rho(\mathbf{x}) f(\mathbf{x}, t) , \quad (2)$$

wherein $f = \partial_t g$. We search for u, \mathbf{v} in a bounded sub-domain Ω of \mathbf{R}^2 with some initial condition at $t = 0$. Considering the mixed first-order formulation instead of the second order wave equation (2) presents two main advantages. Firstly, it can be coupled with the fictitious domain method [13,14] for taking into account the free surface boundary condition. Secondly, it enables us to model wave propagation in infinite domains, the case of interest here, by using the Perfectly Matched absorbing Layer (PML) [15,16]. Note that the PML leads to the elimination of reflections from artificial domain-closure boundaries. The fictitious domain method consists in extending the wave propagation problem in a domain with simple geometry (typically a rectangle in 2D), which enables the use of regular meshes. The free surface boundary condition $\mu \mathbf{n} \cdot \nabla u = 0$ (with \mathbf{n} the unit normal vector to the surface) is then enforced with the introduction of a Lagrange multiplier. This new unknown lives only on the free surface and can be discretized with a non-uniform mesh, different in general from the mesh in the rest of the computation domain (see Fig. 2).

For the space discretization we use a finite element method, whereas for the time discretization a centered second order finite difference scheme is used. The finite elements are

compatible with mass-lumping, which leads to explicit time discretization schemes. For the velocity, we use a new finite element method [17,18] and for the pressure we use P^1 discontinuous functions (this is a different choice from the one in [17,18]). The Lagrange multiplier is discretized with P^1 continuous functions. More details on the numerical method can be found in [13].

The pulse associated with the incident wave is created by a line source of the form

$$g(\mathbf{x}, t) = F(t) \left(1 - \frac{r^2}{r_s^2} \right) \mathbf{1}_{B_s}, \quad (3)$$

where r is the radial coordinate in the x - z plane, and

$$F(t) = \begin{cases} -2\pi v_0^2 [1 - 2\pi v_0^2 (t - t_0)^2] e^{-\pi^2 v_0^2 (t - t_0)^2} & , t \leq 2t_0 \\ 0 & , t > 2t_0 \end{cases}. \quad (4)$$

In the above relations $t_0 = 1/v_0$, v_0 is the central frequency of the spectrum of the pulse, and $\mathbf{1}_{B_s}$ is the characteristic function of the disc B_s , centered at \mathbf{x}_s and with radius r_s . The radial part of $g(\mathbf{x}, t)$ is a smooth approximation to the delta function $\delta(r)$. The radius r_s is small, typically a few discretization steps. In our computations we chose $v_0 = 0.25\text{Hz}$ and $\mathbf{x}_s = (0m, 3000m)$. The densities in the bedrock, soft layer and blocks+foundations were chosen to be: 2000 Kg/m^3 , 1300 Kg/m^3 and 325 Kg/m^3 respectively, whereas the bulk shear wave velocities in these three media were taken to be 600 m/s , 60 m/s and 100 m/s , respectively. The foundation depth of the blocks was $10m$ and the soft layer thickness $50m$. The block widths, heights and separations ranged over $30\text{-}60m$, $50\text{-}70m$, and $60\text{-}100m$ respectively. Most of these parameters are close to those of [12], and are fairly representative of the built features and the substratum at downtown sites in Mexico City. The computational domain was a $3500m \times 3500m$ square (see Fig.2) discretized by a grid of 351 nodes in each dimension (more nodes could be taken to get more computational accuracy and a more detailed description of the motion, notably in the blocks and on the free surface). This domain was surrounded by a PML layer 30 nodes thick, and 465 nodes were placed on the free surface.

To give a measure of the vulnerability of the city, we introduce a so-called vulnerability indices R_j and R_{j+1} . Let T be the time interval of significant shaking (in the computations this was 240 sec). We then define R_j (R_{j+1}) as the ratio between the time-integral from 0 to T of the modulus squared particle velocity ($\partial_t u$) at the center of the summit of the j -th block (at the center of the ground segment between the j -th and $j+1$ -th blocks) and the time integral from 0 to T of the same quantity measured on the ground in absence of all blocks. The subsurface configuration and excitation are the same with or without the blocks.

3 Results

From Fig. 3 we can observe that:

- (i) the duration of shaking is very long (~ 3 min) even for a short (8 sec) input pulse, presumably due to interferences, block/soil interaction and block/soil/block interactions,
- (ii) the motion exhibits a beating phenomenon,
- (iii) the response on the ground is variable (vulnerability indices ranging from 0.69 to 1.28) and very different from that in the no-block configuration, especially as concerns duration,
- (iv) the response at the top of the blocks varies from one block to another, corresponding to vulnerability indices ranging from 1.57 to 2.12 for the ten-block set. This could provide an indication of the destruction of some of the blocks during an earthquake.

The behavior on the ground in between blocks is in agreement with what was found in Ref. 20, and of the same nature as what was observed in various sites in Mexico City.

In order to evaluate the importance of collective effects, we now consider the case of a single block (Fig. 4). At certain instants, the block displacement (the same holds true for the ground displacement in the vicinity of the block (not shown here)) also becomes large, but the motion dies away rather rapidly. This is due to radiation damping [21] (radiation damping also exists in the 10-block case, but is small compared to collective effects such as arise from interference and block/soil/block interactions). In this example, the duration is of the order of 60 sec, which is short relative to the 10-block case, but comparable to the no-block case. The vulnerability index is 1.8, which is larger (by factor 1.8) than the ground response in the absence of the block. This response is quite different from what was observed at most sites overlying soft soil during the earthquakes in cities such as Mexico City.

Other numerical results, not presented here, show that for an incident pulse having a shorter (4 sec) duration, the maximal vulnerability index in the same 10-block city is multiplied by a factor of more than three, while the same overall behavior of response as before manifests itself in terms of duration and spatial variability of shaking. This observation warrants more research on the conditions of optimal coupling of the incident field to the vibrations of the city structure.

4 Conclusions

Most of the most recent attempts to account for anomalous seismic response in cities [5-10] attribute the latter to *complexity in the substratum*. The built features of the cities are not included explicitly in such analyses (i.e., the ground is considered to be flat; see [20] for an exception) and their response is treated separately, using the flat ground motion as the input. Another plausible hypothesis is that irregularities of the free surface and the interface between the foundations and the soft soil, introduced by the existence of built features in a city, may contribute significantly to the overall motion of the site.

We have tested this hypothesis, using a simple 1D-like model of the substratum and a fairly-realistic model of the built environment in a city. An example of ten different non-equally spaced blocks shows that what appears to be due mainly to collective effects accounts for many noticeable features of anomalous response so that the built environment seems to be an important ingredient to obtain realistic predictions of the effects of earthquake in a city. A

similar conclusion was proposed in Ref. 20. When the number of blocks is reduced to one, block/soil/block interactions and interference effects no longer take place so that the main contributing factor to response is the block/soil interaction, resulting from the coupling of vertical resonances of the block with those (of Love modes) of the substratum [11,12,21]. We have shown that this gives rise to relatively modest duration of shaking. However, the peak motion in the block of the one-block situation is often superior to that of some of the blocks in the 10-block configuration. When all the blocks are removed from the model, the response resembles even less the observed responses in the aforementioned cities. This implies that, in order to get qualitative resemblance with the observed responses using our simple model of substratum, it is essential to introduce explicitly more than one block into the model. It seems reasonable to infer from this that including, in explicit manner, a representative sample of the buildings of a city into models with a complex substratum may help to diminish the discrepancy between predicted and observed response in real-life cities.

In the future, in order to analyze and (to predict) earthquake-induced damage in real cities with such models, it will be necessary to i) treat the in-plane motion case, ii) include material losses of the blocks and substratum, iii) extend the analysis to 3D motion, and iv) pay more attention to the seismic source. Based on previous studies concerning the effects of interface irregularities on seismic response [22,23], we do not expect to see significant qualitative differences between in-plane and out-of-plane motion in structures such as those studied herein. As concerns 3D as opposed to 2D models, it has been suggested [21] that 2D models underestimate real (i.e., 3D) seismic response due to overestimation of radiation damping. The effect of the inclusion of material losses can be anticipated by reference to what occurs in the forced motion of a 1D oscillator [23]: exponential reduction of the motion at a rate proportional to the inverse of the quality factor (the latter being infinite in the absence of material losses). This means that we anticipate results that exhibit a shortening of the duration of motion with respect to what was shown herein, but since our durations were very long (~ 3 min), it is probable that the more realistic structural models will result in durations of the order of those found by Gueguen et al. [20] with their 3D structural model including material losses (however, this model is approximate in nature as concerns the interaction of the seismic wave with the city).

Acknowledgements

This research was carried out within the framework of the Action Concertée Incitative “Prévention des Catastrophes Naturelles” entitled “Interaction 'site-ville' et aléa sismique en milieu urbain” of the French Ministry of Research.

Bibliographic references

- [1] EQE: The January 17, 1995 Kobe Earthquake, EQE Summary Report, April 1995, <http://www.eqe.com/publications/kobe/kobe.htm>.
- [2] Mucciarelli M., Camassi R. & Gallipoli M.R.: The Izmit (Turkey) 1999 earthquake, http://www.pz.cnr.it/imaaa/turchia/report_e.html.
- [3] Semblat J.-F., Duval A.-M. & Dangla P.: Numerical analysis of seismic wave amplification in Nice (France) and comparisons with experiments. *Soil Dynam.Earthqua.Engrg.* **19**, 347-362, 2000.

- [4] Singh S.K., Mori A., Mena E., Krüger F. & Kind R. : Evidence for anomalous body-wave radiation between 0.3 and 0.7 Hz from the 1985 september 19 Michoacan, Mexico earthquake, *Geophys.J.Int.* **101**, 37-48, 1990.
- [5] Chavez-Garcia F.J. & Bard P.-Y.: Site effects in Mexico City eight years after the September 1985 Michoacan earthquakes, *Soil Dyn.Earthquake Engrg.* **13**, 229-247 , 1994.
- [6] Bard P.-Y., Eeri M., Campillo M., Chavez-Garcia F.J. & Sanchez-Sesma F.J. : The Mexico earthquake of September 19, 1985--a theoretical investigation of large-and small-scale amplification effects in the Mexico City valley, *Earthquake Spectra*, **4**, 609-633, 1988.
- [7] Olsen K.B.: Site Amplification in the Los Angeles Basin from Three-Dimensional Modeling of Ground Motion, *Bull.Seism.Soc.Am.*, **90**, 77 – 94, 2000.
- [8] Hartzell S., Cranswick E., Frankel A., Carver D. & Meremonte M.: Variability of site response in the Los Angeles urban area, *Bull.Seism.Soc.Am.*, **87**, 1377-1400, 1997.
- [9] Wald D.J. & Graves R.W.: The seismic response of the Los Angeles Basin, California, *Bull.Seism.Soc.Am.*, **88**, 337-356, 1998.
- [10] Burridge R. : Soil amplification of plane seismic waves, *Phys.Earth Planet Int.*, **22**, 122-136, 1989.
- [11] Wirgin A.: Love waves in a slab with rough boundaries, in *Recent Developments in Surface Acoustic Waves*, Parker D.F. & Maugin G.A. (eds.), Springer, Berlin, 145-155, 1988.
- [12] Wirgin A. & Bard P.-Y.: Effects of buildings on the duration and amplitude of ground motion in Mexico City, *Bull.Seism.Soc.Am.*, **86** , 914-920, 1996.
- [13] Tsogka C., *Modélisation mathématique et numérique de la propagation des ondes élastiques tridimensionnelles dans des milieux fissurés*, Thèse de Doctorat, Université Paris IX Dauphine, Paris, 1999.
- [14] Bécache E., Joly P. & Tsogka C.: Application of the fictitious domain method to 2D linear elastodynamic problems, *J.Comput.Acoust.* **9**, 1175-1202, 2001.
- [15] Bérenger J.P. A perfectly matched layer for the absorption of electromagnetic waves, *J.Comput.Phys.* **114**, 185-200, 1994.
- [16] Collino F. & Tsogka C.: Application of the PML absorbing layer model to the linear elastodynamic problem in anisotropic heterogeneous media, *Geophys.* **66**, 294-307, 2001.
- [17] Bécache E., Joly P. & Tsogka C.: Etude d'un nouvelle élément fini mixte permettant la condensation de masse, *C.R.Acad.Sci.Paris Sér.I Math.* **324**, 1281-1286, 1997.
- [18] Bécache E., Joly P. & Tsogka C.: An analysis of new mixed finite elements for the approximation of wave propagation problems, *SIAM J.Numer.Anal.* **37**, 1053-1084, 2000.
- [19] Wirgin A. & Kouoh-Bille L. : Amplification du mouvement du sol au voisinage d'un groupe de montagnes de profil rectangulaire ou triangulaire soumis à une onde sismique SH, in *Génie Parasismique et Aspects Vibratoires dans le Génie Civil*, AFPS, Saint-Rémy-lès-Chevreuse, ES-28--ES-37, 1993.
- [20] Gueguen P., Bard P.-Y. & Chavez-Garcia F.J. : Site-city seismic interaction in Mexico City like environments : an analytic study, *Bull.Seism.Soc.Am.* **92**, 794-804, 2002 .
- [21] Wolf J.P.: *Vibration Analysis Using Simple Physical Models*, Prentice-Hall, Englewood Cliffs, 1994.
- [22] Hill N.R. & Levander A.R.: Resonances of low-velocity layers with lateral variations, *Bull.Seism.Soc.Am.* **74**, 521-537, 1984.
- [23] Levander A.R. & Hill N.R.: P-SV resonances in irregular low-velocity surface layers, *Bull.Seism.Soc.Am.* **75**, 847-864, 1984.

- [24] Capra A. & Davidovici V.: *Calcul Dynamique des Structures en Zone Sismique*, Eyrolles, Paris, 1980.

Figure captions

Figure 1. Sagittal plane view of the 2D structure. The thick black curve is the stress-free boundary above which is air. The grey regions are (from top to bottom): the blocks with foundations, underlaid by a soft layer and the bedrock half-space. The dashed black lines are the foundation boundaries.

Figure 2. A schematic view of the grid used in the soil/air region (light and dark gray regions) and on the free surface (segments with dots). The nodal points on the free surface do not necessarily coincide with nodal points of the soil+air region. The number of points in both of these sets is considerably larger in the actual computations than in this drawing.

Figure 3. Time records of total particle velocity of a set of ten blocks. Each row of the figure depicts the particle velocity (in m/sec): at the center of the top of the j -th block (left), the center of the ground segment between the j -th and $(j+1)$ -th block (middle) and the $(j+1)$ -th block (right). Here j ranges from 5 to 10 (top to bottom). The solid curves in all the subfigures represent the particle velocity at ground level in the absence of blocks. The vulnerability indices R_j at the top of the j -th block and R_{j+1} on the ground between the j -th and $j+1$ -th blocks, are indicated at the top of each subfigure. The abscissas designate time, and range from 0 to 250 sec . Note that the scales of the ordinates vary from one subfigure to another.

Figure 4. Time records of total particle velocity for a 'city' with only one block ($h=50m$, $w=30m$). The two curves correspond to the particle velocity at ground level in the absence of the block (solid curve) and at the center of the top of the block (dashed curve).

Légendes des figures

Fig.1 Représentation, dans le plan sagittal, de la structure 2D. La courbe noire épaisse désigne la frontière libre au-dessus de laquelle se trouve de l'air. Les régions grises (de haut en bas) désignent: les blocs avec fondations, la couche superficielle molle, et le massif rocheux. Les segments en tirets désignent les frontières des fondations.

Fig.2 Vue schématique de la grille employée dans la région sous-sol+air (parties claires et grises) et sur la surface libre (segments avec points). Les points nodaux sur la surface libre ne coïncident pas nécessairement avec les points nodaux de la région sous-sol+air. Le nombre de points dans chacun de ces ensembles est considérablement plus important dans les calculs que dans le dessin.

Fig. 3 Enregistrements temporels de la vitesse totale particulière pour un groupe de dix blocs. La courbe discontinue dans chaque sous-figure désigne la vitesse particulière (en m/sec) au centre de la face supérieure du j -ième bloc. Ici j varie de 5 à 10 (en allant du haut vers le bas). Les courbes continues dans toutes les sous-figures représentent la vitesse particulière au niveau du sol en l'absence des blocs. Les indices de vulnérabilité R_j au sommet du j -ième bloc, et R_{j+1} au sol entre les j -ième et $j+1$ -ième blocs, sont indiqués en haut de chaque panneau. Les abscisses désignent le temps, et varient de 0 à 250 sec . On remarque que l'échelle des ordonnées varie d'une sous-figure à l'autre.

Figure 4. Enregistrements temporels de la vitesse totale particulaire au voisinage d'un seul bloc (au sommet: courbe en pointillés) et en l'absence de ce bloc (au sol: courbe continue). Les paramètres du bloc sont $h=50m$, $w=30m$.

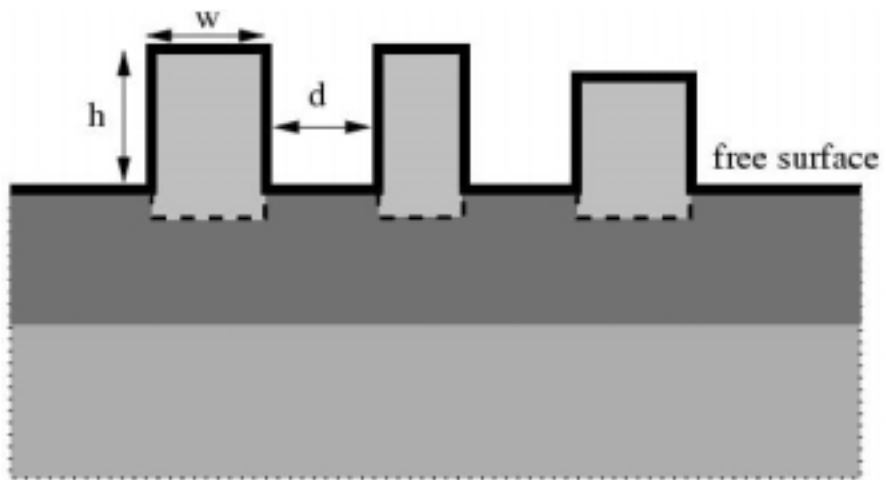


Figure 1. (Tsogka et Wirgin)

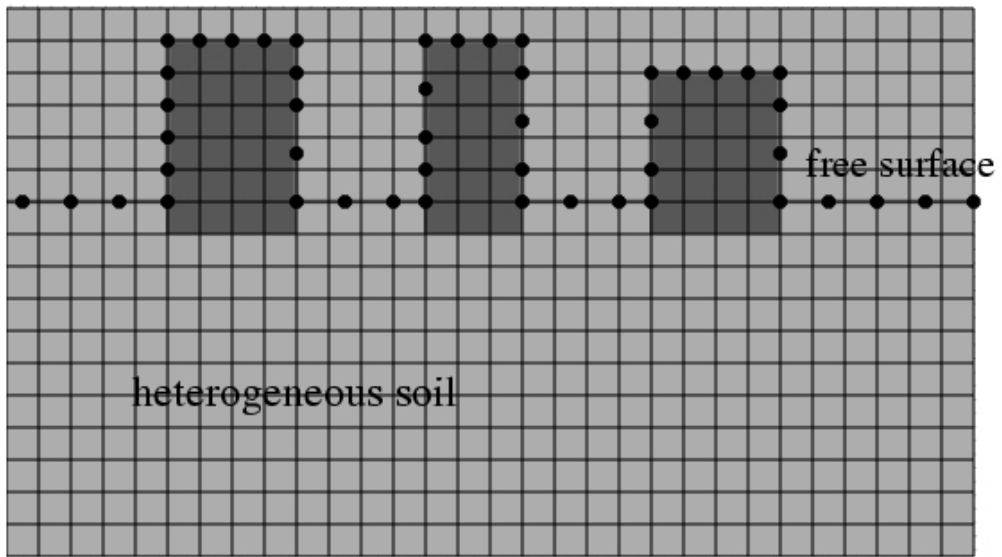


Figure 2. (Tsogka et Wirgin)

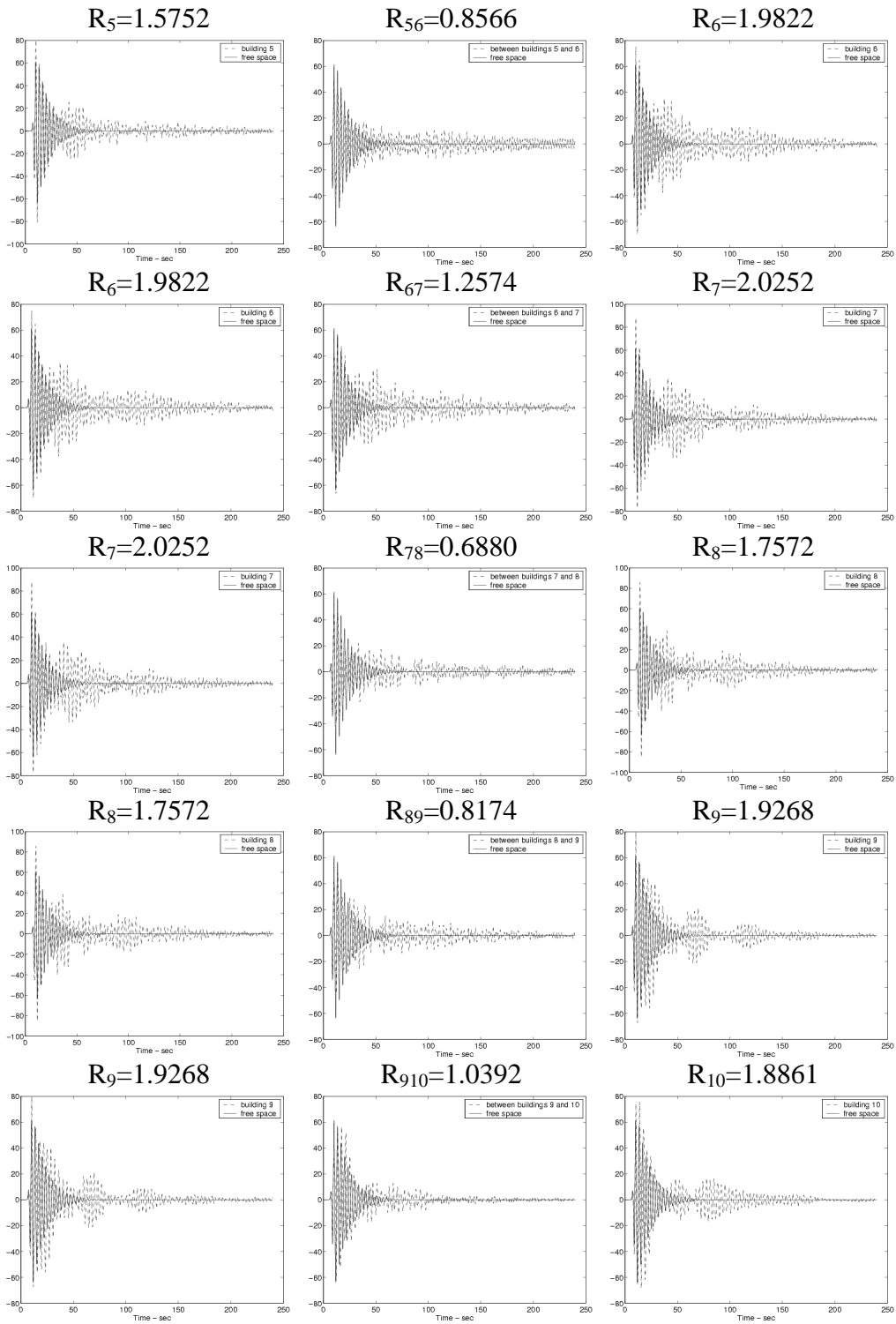


Figure 3. (Tsoyka et Wirgin)

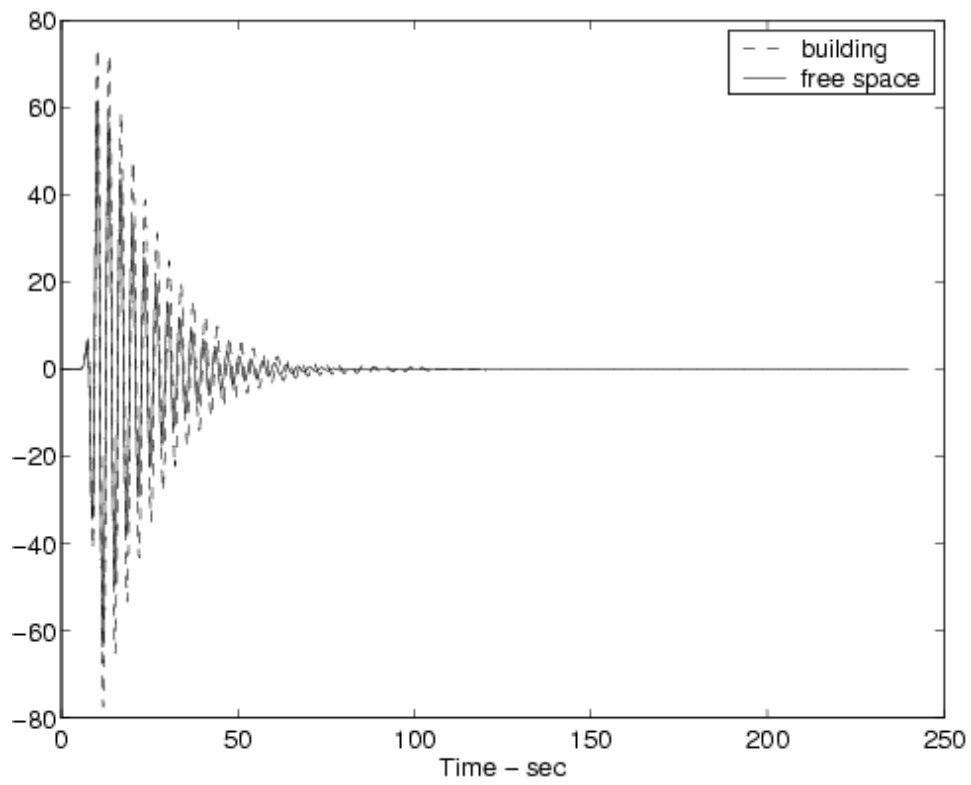


Fig. 4 (Tsogka et Wirgin)